

## Annual and diurnal water vapor cycles at Curiosity from observations and column modeling

Hannu Savijärvi<sup>1,2,\*</sup>, Timothy H. McConnochie<sup>3,4</sup>, Ari-Matti Harri<sup>2</sup>, Mark Paton<sup>2</sup>

<sup>1</sup>Institute for Atmospheric and Earth System Research / Physics, University of Helsinki, Finland

<sup>2</sup>Finnish Meteorological Institute, Helsinki, Finland

<sup>3</sup>Department of Astronomy, University of Maryland, College Park, MD20742, United States

<sup>4</sup>NASA Goddard Space Flight Center, Greenbelt, MD20771, United States

revised 5.10.2018

### Abstract

Local column precipitable water contents (PWC) for more than a martian year from 113 Curiosity ChemCam passive-mode sky scans were used to force a column model with subsurface adsorption. ChemCam volume mixing ratios (vmr) and T, RH and vmr from REMS-H were compared with model results. The REMS-H observations point to decrease of vmr (i.e. depletion of near-surface water vapor) during every evening and night throughout the year. The model's pre-dawn results are quite similar to the REMS-H observations, if adsorption is allowed. The indicated porosity is about 30% and the night depletion ratio about 0.25. If adsorption is not allowed, RH and vmr become excessive during every night at all seasons, leading to ground frost between Ls 82°-146°; frost has not been observed. As brine formation is unlikely along the Curiosity track, adsorption thus appears to be the depleting process.

During daytime the ChemCam vmr is in general close to surface values from the Mars Climate Database (MCD) vmr profiles for the Curiosity site when those profiles are scaled to match the ChemCam PWC. Our simulated daytime surface-vmr is in turn close to the ChemCam vmr when moisture is assumed well-mixed to high altitudes, whereas a low moist layer (15 km) leads to overestimates, which are worse during the warm season. Increased TES-like regional PWC also leads to large overestimates of daytime surface-vmr. Hence the crater appears to be drier than the region surrounding Gale and the results support a seasonally varying vertical distribution of moisture with a dry lower atmosphere (by Hadley circulation), as suggested by MCD and other GCM experiments.

Keywords: Mars, climate      Mars, surface      Meteorology

\*Corresponding author at: INAR/Physics, Faculty of Science, 00014 University of Helsinki, Finland

E-mail address: [hannu.savijarvi@helsinki.fi](mailto:hannu.savijarvi@helsinki.fi)

Tel: +358-40-9380858

## 48 1. Introduction

49  
50 The martian water cycle has been the object of intense research through orbit observations and  
51 general circulation model experiments (GCM), reviewed recently by Montmessin et al. (2017).  
52 Martinez et al. (2017) reviewed all surface-based observations. Among the less well-known aspects  
53 of the water cycle are the surface interactions and the vertical distribution of moisture, both being  
54 difficult to observe. This article is an attempt to study them via the Mars Science Laboratory (MSL)  
55 observations onboard the Curiosity rover in the Gale crater. We use the ChemCam passive-mode  
56 sky scans for column precipitable water content (PWC, McConnochie et al., 2018) and the Rover  
57 Environmental Monitoring Station humidity measurements (REMS-H, Harri et al., 2014a, Gomez-  
58 Elvira et al., 2012) during more than one martian year (MY). A column model is applied to help  
59 interpret the observations.

60  
61 According to GCM experiments and data assimilations (Richardson and Wilson, 2002; Navarro et  
62 al., 2014; Steele et al., 2014; Mars Climate Database (MCD, Millour et al., 2015); Montmessin et  
63 al., 2017) the equatorial latitude of Gale (4.6°S) is relatively dry near the surface throughout most of  
64 the martian year, because of transport by the large-scale Hadley circulation. High mixing ratios of  
65 water vapor would hence be expected aloft, at 10-15 km during the cool aphelion season ( $L_s \sim 71^\circ$ )  
66 and at 30-40 km during the warm perihelion season ( $L_s \sim 251^\circ$ ), but these model predictions have  
67 been hard to prove by observations. The moist season of high PWC would occur at Gale at around  
68  $L_s 180^\circ$ , when the water vapor pulse from the sublimated north polar ice cap finally reaches the  
69 equatorial latitudes.

70  
71 At the surface, the possible exchange of water with the surface has been debated since the Viking  
72 observations, which according to Jakosky et al. (1997) displayed depletion of near-surface water  
73 vapor each night that was not due to formation of frost. They suggested and modeled regolith  
74 adsorption as the reason. Evening depletion has been reported in the TECP data of Phoenix (Zent et  
75 al., 2016) and depletion is present in REMS-H data (Harri et al., 2014a, Savijärvi et al., 2015).  
76 Surface brine formation might also deplete air moisture (Martin-Torres et al., 2015) but this is not  
77 favored by Curiosity data (Rivera-Valentin et al., 2018). Savijärvi et al. (2016, 2017) used a column  
78 model with adsorption and frost to explain the first-sols observations of Viking and Curiosity. Steele  
79 et al. (2017) applied an adsorptive mesoscale model for the Gale region but they, too, considered  
80 just a few sols, although during the three main seasons.

81  
82 Here observations and the column model with and without adsorption are used to study the diurnal  
83 and annual cycles of water vapor at Curiosity. The model is forced by the rover's strictly local  
84 ChemCam daytime PWC through more than one martian year, and the REMS-H observations and  
85 model results for diurnal temperatures, relative humidities and mixing ratios are compared at the  
86 observation height of 1.6 m. Two vertical profiles for the model's initial mixing ratio are tested.  
87 Furthermore, increased values of PWC, closer to the regional orbit retrievals by TES and CRISM  
88 over Gale, are tried for comparison.

89  
90 Observations and model experiments are described in Section 2. Section 3 demonstrates the diurnal  
91 cycles during the warm season, and Section 4 respectively during the cool season (the moist season  
92 was discussed in Savijärvi et al., 2016). The full annual cycle is then considered in Section 5 and  
93 the findings are discussed in Section 6. Conclusions are given Section 7.

## 94 95 96 2. Observations and model experiments

97  
98 The MSL ChemCam passive spectroscopic scans of scattered skylight can be used to provide local  
99 estimates of column precipitable water content (PWC) and the dust and water ice fractions of the

100 total 880 nm aerosol optical depth  $\tau$  from MastCam, given the surface pressure  $p$ , which is  
 101 measured by the MSL REMS-P device (Harri et al., 2014b). The methodology and first results are  
 102 described in McConnochie et al. (2018). We use their results, which originate from 113 ChemCam  
 103 passive sky scans from MSL sols 230-1293 (Ls 291° MY31 to Ls 127° MY33). The scans are  
 104 mostly from daytime, between 10-13 Mars hours local mean solar time (LT); some are from the  
 105 morning, 07-09LT. The indicated precision for PWC is  $\pm 0.6 \mu\text{m}$ . We assume in the following that  
 106 the ChemCam values represent the strictly local conditions along the Curiosity track on the Gale  
 107 crater base.

108  
 109 The simultaneous measurements of PWC,  $\tau$  (mostly due to dust) and  $p$  are shown in Figure 1 as  
 110 function of season. Since  $\tau$  and  $p$  are not originally simultaneous with the ChemCam PWC scans,  
 111 we apply the same interpolation procedure that was used by McConnochie et al. (2018). One may  
 112 note low PWC and dustiness during the cool aphelion – southern late fall season at around Ls 71°-  
 113 90°, a moist season with high PWC and low  $p$  at around Ls 180°, and a long dusty mid-PWC period  
 114 during the warm perihelion – southern late spring, Ls 251°-270°. The few morning values are  
 115 similar to the surrounding daytime PWC retrievals, indicating little or no diurnal variation of PWC.  
 116

117 These local ChemCam PWC retrievals, when scaled to the traditional reference  $p$  of 6.1 mb, appear  
 118 consistently lower by 2-4  $\mu\text{m}$  than the similarly-scaled regionally averaged retrievals from TES and  
 119 CRISM in McConnochie et al. (2018). The large averaging area for the orbital data sets spanned 40  
 120 degrees of longitude and 10 degrees of latitude. When CRISM averaging was restricted to a local  
 121 scale covering only the interior of the Gale crater (Toigo et al., 2013), the resulting lower PWCs  
 122 become consistent with ChemCam. This suggests that low daytime PWCs are a real feature of the  
 123 crater rather than some kind of instrumental bias. In the Steele et al. (2017) high-resolution  
 124 simulations daytime upslope winds flush the desorbed moisture out of the crater base (cf. their figs.  
 125 15h, 16f), thus keeping the crater relatively dry during all the three seasons they considered.  
 126

127 The MSL REMS-H device onboard Curiosity consists of a fast temperature sensor and three relative  
 128 humidity Vaisala sensors in a dust-protected cage 1.6 m above the surface (Harri et al. 2014a). We  
 129 use here the hourly 5 min averages of  $T$  and the first hourly measurements of RH of selected sols  
 130 (data from the Planetary Data System). The value for the volume mixing ratio of water vapor at 1.6  
 131 m (vmr) is calculated from the observed  $p$ ,  $T$  and RH ( $\text{vmr} = \text{RH} \cdot e_{\text{sat}}(T)/p$ ;  $e_{\text{sat}}$  is the saturation  
 132 pressure of water vapor with respect to ice) as in Savijärvi et al. (2016). Because the cage is well-  
 133 ventilated, the REMS-H temperatures closely follow the free air temperature at 1.6 m. Values for  
 134 RH and vmr are most accurate at maximum RH (minimum vmr). This typically occurs daily during  
 135 nighttime, at 04-06LT (cf. Figures 3-4). During daytime RH is very small ( $< 2\%$ ) and the REMS-H  
 136 -derived values for vmr unfortunately become unreliable.  
 137

138 The column model is the same as used for MSL and described in detail in Savijärvi et al. (2016)  
 139 with two small refinements explained below. The atmospheric part is hydrostatic with constant  
 140 geostrophic wind of 10 m/s (leading to near-surface winds of about 2 m/s at nighttime and about 5  
 141 m/s during daytime). There are 29 levels from 0.3, 0.7, 1.6, 7 m ... to 50 km. Parameterizations  
 142 include radiation, turbulence and interactive cloud physics. Subsurface vertical diffusion of soil  
 143 temperature and pore volume moisture with possible adsorption of moisture on regolith grains is  
 144 represented in eight levels from the surface down to 48 cm depth. Adsorption isotherm follows the  
 145 Jakosky et al. (1997; J97) formulation. Icefog, iceclouds, surface frost and pore ice form during  
 146 supersaturation and sublimate under subsaturation with the associated latent heat and radiative  
 147 effects.  
 148

149 The two refinements to the Savijärvi et al. (2016) regolith scheme are as follows:  
 150

151 1) The coefficient  $D$  for molecular/Knudsen diffusion of water vapor in  $\text{CO}_2$  pore volume gas,

152 which was  $1 \text{ cm}^2/\text{s}$ , is increased to  $5 \text{ cm}^2/\text{s}$ , based on test chamber experiments in martian  
 153 pressures, temperatures and regolith representations of Hudson et al. (2007). The diurnal  
 154 minima and maxima of vmr do not change by this but the late morning and early evening  
 155 behavior is closer to the recalibrated Phoenix TECP results of Fischer et al. (2018).

- 156 2) The scaled diffusion coefficient during active adsorption  $D'$  is no longer constant but is  
 157 allowed to vary with the predicted regolith temperature and pore space moisture at each  
 158 depth. The effect of this is small as  $D'$  and its variations with temperature and moisture are  
 159 quite small,  $D' \sim 3 \cdot 10^{-6} \text{ cm}^2/\text{s}$ .

160  
 161 In the present Curiosity simulations thermal inertia is 300 SI units, surface albedo 0.18, surface  
 162 roughness length 1 cm and regolith porosity 0.3 for simplicity, even though these may vary in  
 163 reality along the track. The model is initialized at 00LT for each Ls of Figure 1 from the observed  
 164 PWC,  $\tau$  and  $p$  (with dust well-mixed and  $T$  210K at the surface, lapsing 1 K/km). It is then run to  
 165 sol three with  $p$  and  $\tau$  constant, by which time its winds, temperatures and mixing ratios have spun  
 166 up at all heights to a repeating diurnal cycle, which closely preserves the initial PWC (for porosity  
 167 of 0.3). The model values shown are from this last sol.

168  
 169 Initialization of the unknown moisture profile to the ChemCam PWC is made using two simple  
 170 alternatives. The first is a high-layered well-mixed assumption (“well-mixed”), in which the water  
 171 vapor mixing ratio is the same at all heights up to 50 km. The other assumes a 15 km high well-  
 172 mixed layer, above which vmr decays to zero (“low moist layer”). This is based on GCM cool-  
 173 season results (e.g. Montmessin et al., 2017, fig. 11.18), in which moisture at the equatorial latitudes  
 174 appears concentrated nearer the surface, maximum vmr being typically at around 10-15 km height  
 175 with a rapid decay aloft. To obtain the same ChemCam PWC, vmr must now be about 26% higher  
 176 in this low layer than in the high layer case. The well-mixed assumption might be expected to be  
 177 better during the warm season and the low moist layer assumption during the cool season. The pore  
 178 volume mixing ratio is initialized to the boundary layer mean (~4 km) of the initial air mixing ratio  
 179 in each experiment. Cloud processes are switched off above 7 km (the well-mixed profile would  
 180 lead to extreme cool season supersaturations at high altitudes), but fogs and boundary layer clouds  
 181 are allowed to occur as in the Viking and Phoenix simulations of Savijärvi et al. (2010, 2017).  
 182 However, they do not occur in any of the present integrations, due to the fairly dry equatorial Gale  
 183 environment.

184  
 185 Two further experiments are made using the well-mixed initial moisture. As the strictly local  
 186 ChemCam results for PWC appear consistently 2-4  $\mu\text{m}$  lower than the large-scale regional TES and  
 187 CRISM retrievals (McConnochie et al., 2018), we trace the sensitivity of our results to this by  
 188 increasing all the ChemCam PWC values by 4  $\mu\text{m}$ . In a fourth experiment adsorption is set to zero,  
 189 but vertical diffusion of moisture remains active in the porous regolith. There are thus four  
 190 simulations for each PWC observation of Figure 1: well-mixed (“wm”), low moisture layer (“low  
 191 m”), increased moisture (“high pwc”), and no adsorption (“no ads”).

192  
 193 Figure 2 displays for later reference the model’s 1.6 m temperatures at 05LT and at the scan hour of  
 194 each observation of Figure 1. The model temperatures are practically the same in all four  
 195 experiments and are quite close to the respective REMS-H observations (Figures 3-4). Figure 2  
 196 indicates that the morning ChemCam scans are mostly from around 08LT (with one at 09:00LT and  
 197 one at 07:15LT). The 102 daytime observations are mostly from around 11LT and 12LT, with a few  
 198 around 10LT and 13LT. The cool and warm seasons are clearly visible in Figure 2 and the moist  
 199 season in Figure 1.

### 202 3. Diurnal comparison during the warm season

203

204 First comparisons between the REMS-H observations and the adsorptive column model results  
 205 were made in Savijärvi et al. (2016) for MSL sols 15-17 and 80-82 during the moist season. The  
 206 model was initialized at  $L_s$  159° and 196° with an approximate PWC of 9.3  $\mu\text{m}$  and 8  $\mu\text{m}$ ,  
 207 respectively. Results indicated good matches for diurnal temperatures and relative humidities at 1.6  
 208 m. A fair match with the REMS-H mixing ratios was obtained during the early morning hours. In  
 209 this section the observed and modeled diurnal cycles are similarly compared during the warm  
 210 season.

211  
 212 Figure 3 displays hourly REMS-H observations for three sols at around  $L_s$  271° and the model's  
 213 diurnal cycle arising from ChemCam MY32  $L_s$  270.96° 10:20LT scan, PWC being 7.45  $\mu\text{m}$ ,  $\tau$  0.87  
 214 with dust fraction 0.83, and  $p$  9.20 mb. The observed  $T$  (top panel) ranges between 205-273K. The  
 215 model's  $T$  at 1.6 m is quite close to the observations. Model's surface temperature  $T_s$  is also  
 216 displayed.

217  
 218 The observed relative humidities (mid panel) are small, reaching only to 6-9% near sunrise. The  
 219 two model experiments with the ChemCam PWC (well-mixed: thick line, low moist layer: thin line)  
 220 are on the low side of the REMS-H observations, whereas values from the increased-PWC  
 221 experiment (11.5  $\mu\text{m}$ , dotted line) are here rather good. RH from the no-adsorption experiment  
 222 (dashed line) is clearly too high in the morning.

223  
 224 The REMS volume mixing ratios (bottom panel) decline during the late evening and night until  
 225 sunrise, indicating some depleting process. The three simulations with adsorption produce values  
 226 quite close to the observed 05-06LT minima of vmr, roughly covering the sol-to-sol range of 20-40  
 227 ppmv. The depleted layer of moisture is quite shallow, only 100-200 m (Savijärvi et al., 2016), so  
 228 the column-PWC does not change notably during the sol. In the no-adsorption simulation (dashed)  
 229 vmr is effectively constant during the sol, even though vertical diffusion of moisture is active both  
 230 in the air and in the regolith. This leads to excessively high RH and vmr at nighttime. Hence the  
 231 nocturnal diffusion into the soil is alone (i.e. without adsorption) not an effective remover of air  
 232 moisture in the diurnal timescale.

233  
 234 The mixing ratios increase after sunrise (in the model due to desorption, upward diffusion and  
 235 convection). The REMS-H values for vmr are unfortunately unreliable during daytime (because of  
 236 very small, inaccurate RH), but the ChemCam vmr (72 ppmv at 10:20 LT) provides here a kind of  
 237 validation. ChemCam vmr estimates come from applying a well-mixed assumption to the  
 238 ChemCam PWC (McConnochie et al., 2018), and they may actually be quite accurate near the  
 239 surface, as will be discussed in Section 6. ChemCam vmr is in Figure 3 close to the well-mixed  
 240 model's vmr curve (thick line), which grows to about 90 ppmv in the afternoon. The experiment  
 241 with a low moist layer (thin line) leads to slightly higher vmr, and the one with increased PWC  
 242 (11.5  $\mu\text{m}$ , dotted) even higher, vmr then growing up to 140 ppmv in the afternoon. Adsorption  
 243 begins to strongly deplete the near-surface moisture from about 16LT onward in all the three  
 244 simulations with adsorption.

245  
 246 Steele et al. (2017) presented mesoscale model simulations for Gale at around  $L_s$  321° within the  
 247 warm season. The TES MY26 data-assimilated initial PWC was about 10  $\mu\text{m}$  over the Gale region.  
 248 Their results with the J97 adsorption (fig. 24) indicate at the MSL site a surface vmr of about 40  
 249 ppmv at 06LT and about 100 ppmv at 16LT, not too different from the above warm season  
 250 observations and column model results.

#### 253 4. Diurnal comparison during the cool season

254  
 255 Figure 4 displays comparisons for  $L_s$  90° within the cool season, the ChemCam-observed local

256 PWC being  $5.31 \mu\text{m}$  with  $\tau$  0.41 (dust fraction 0.84) and  $p$  8.44 mb at Ls  $89.93^\circ$ , 11:43 LT, MY32.  
 257 The REMS-H temperatures for three sols around Ls  $90^\circ$  (top panel) are about 20K lower than at Ls  
 258  $271^\circ$ , with some sol-to-sol scatter. The model's T1.6m values match the nighttime and morning  
 259 REMS-H observations again quite well but the afternoon T-maximum remains too cold. The three  
 260 simulations with adsorption indicate here air frost points  $T_f$  below the air and ground temperatures,  
 261 so no frost nor fog is expected. However, in the no-adsorption simulation,  $T_f$  does hit the surface  
 262 temperature at around 02LT and ground frost is thereafter deposited until sunrise.

263  
 264 The observed nighttime maxima of relative humidity at 04-06LT are here in the range of 30-45%  
 265 with wide sol-to-sol scatter. Adsorptive simulations with ChemCam local PWC (thin and thick solid  
 266 lines) again display RH on the low side of REMS-H observations, whereas that with increased  
 267 PWC (dots) appears on the high side. The same holds for the nocturnal 01-07LT mixing ratios,  
 268 which are now quite low (10-15 ppmv), displaying only little sol-to-sol scatter.

269  
 270 The ChemCam vmr of 56 ppmv at 11:43LT is here located between the well-mixed and low moist  
 271 layer simulation curves. Increased PWC ( $9.3 \mu\text{m}$ , dotted) provides on the other hand daytime values  
 272 of vmr, which are much higher, up to 95 ppmv. In the no-adsorption experiment (dashed), formation  
 273 of ground frost depletes the near-surface vmr from 02LT onward. After sunrise rapid sublimation of  
 274 frost returns the deposited moisture back to the air, increasing vmr temporarily at around 08LT near  
 275 the surface.

276  
 277 In Steele et al. (2017) the cool season simulation (their fig. 28, Ls  $69^\circ$ ; PWC about  $7 \mu\text{m}$  over Gale)  
 278 indicates surface-vmr of about 20 ppmv at 06LT and 80 ppmv at 16LT at the MSL site, again rather  
 279 consistent with the above observations and column model results.

280  
 281

## 282 5. The annual cycle

283  
 284 Results from the annual cycle simulations are displayed in two parts for clarity. Figure 5 shows all  
 285 the ChemCam daytime vmr values for the cool season (Ls  $0^\circ$ - $135^\circ$ ), together with the model's  
 286 respective 1.6 m vmr at the ChemCam observation time, and at 05:00LT (the typical hour of  
 287 minimum vmr). The two model daytime values are from the ChemCam PWC-forced simulations  
 288 with adsorption, for the well-mixed and low moist layer assumptions. Simulations with increased  
 289 PWC produced quite high vmr values (not shown), which are consistently about 50 ppmv above the  
 290 ChemCam vmr, as was demonstrated in Figures 3-4.

291  
 292 In Figure 5 the lowest values of daytime ChemCam vmr occur at around Ls  $30^\circ$ - $70^\circ$ , as discussed in  
 293 McConnochie et al. (2018), and not during the coldest sols, which occur around Ls  $90^\circ$  (Figure 2).  
 294 The ChemCam vmr then increase toward Ls  $135^\circ$ . Well-mixed model's vmr values (\*) are typically  
 295 slightly lower than the ChemCam vmr, whereas the low moist layer experiments (+) tend to  
 296 overestimate for higher vmr. At 05LT the model's vmr values are consistently quite low, due to  
 297 depletion by adsorption in a shallow layer near the surface, as were the REMS-H observations in  
 298 Figure 4.

299  
 300 Frost did not form in any of the simulations with adsorption, not even with increased PWC.  
 301 However, when adsorption was switched off, frost did occur every night during Ls  $86^\circ$ - $142^\circ$ . Frost  
 302 has not been observed so far along the Curiosity track (Martinez et al., 2016, 2017), giving further  
 303 support to the adsorption assumption for the nocturnal depletion.

304  
 305 Figure 6 similarly covers the warm season, Ls  $135^\circ$ - $360^\circ$ . It is rather unfortunate that the probably  
 306 most humid period at around Ls  $160^\circ$ - $190^\circ$  did not have any ChemCam sky scans. After about Ls  
 307  $210^\circ$  the vmr values stay rather steady at 50-100 ppmv with a weak decline toward Ls  $360^\circ$ . The

308 well-mixed model's values of vmr at 1.6 m are here close to the ChemCam vmr, whereas the low  
 309 moist layer experiments produce values, which are higher by 20-40 ppmv, and the increased PWC  
 310 simulations (not shown), by about 50 ppmv.

311  
 312 The model's 05LT vmr values are consistently much lower than vmr at 10-13LT in Figures 5-6. The  
 313 respective night depletion ratio  $R = \text{vmr}(05\text{LT})/\text{vmr}(\text{daytime})$  is plotted in Figure 7, using the  
 314 ChemCam and model's 10-13LT vmr. It is seen that  $R$  is nearly constant and about 0.25 throughout  
 315 the martian year, with lowest values during the cool season and highest values during the moist  
 316 season. Excessive values of model- $R$  (e.g. at Ls 82° and at Ls 315°) may partly be due to the early  
 317 ChemCam scans (around 10LT, Figure 2), when desorption has not yet been operating for long in  
 318 the model. Hence the model-vmr at 1.6 m is about 20% lower at 10LT than it will be during midday  
 319 (Figures 3-4), whereas the ChemCam vmr is based on the column-PWC, which does not display  
 320 strong diurnal variation (Figure 1).

321

322

## 323 6. Discussion

324

325 In Figure 4 from the cool season there are considerable sol-to-sol variations at 00-05LT in the  
 326 observed high and thus relatively accurate REMS-H relative humidities. They are anti-correlated  
 327 with the respective sol-to-sol variations in the temperatures (e.g. at 00LT and 05LT). The low  
 328 volume mixing ratios exhibit on the other hand only little sol-to-sol variation in this season in  
 329 Figure 4 (and in Martinez et al., 2017), mainly because the anti-correlated variations of RH and T  
 330 tend to compensate each other in the evaluation of vmr. One may thus suspect that the low  
 331 nocturnal absolute humidity at Curiosity is much the same from sol to sol during the cool season.  
 332 Therefore any sol-to-sol changes in temperatures (perhaps due to weak local advection effects) are  
 333 immediately carried on to the relative humidities. This also implies that REMS-H is measuring air  
 334 temperatures and relative humidities independently and fairly accurately during the night.

335

336 In contrast, during the warm season the observed hourly 01-06LT temperatures (and thus  $e_{\text{sat}}(T)$ ) are  
 337 much the same from sol to sol, by Figure 3. Hence the large observed sol-to-sol variations in the  
 338 high vmr during the warm season lead to relatively large sol-to-sol variations around the small RH,  
 339 as seen in Figure 3 and in Martinez et al. (2017).

340

341 In general the REMS-H observations display a clear depletion of near-surface absolute moisture in  
 342 the evening and night during all seasons along the Curiosity track, by some process or processes.  
 343 This prevents frost. Our column model with adsorption is on the other hand close to the ChemCam-  
 344 observed daytime vmr and to the pre-dawn much smaller REMS-H-observed vmr, whereas the no-  
 345 adsorption experiments produce too high vmr at night. Hence adsorption is likely at Gale  
 346 throughout the year.

347

348 When adopting higher PWC mimicking the large-scale TES and CRISM retrievals for Gale (Mc  
 349 Connochie et al., 2018), both our column model and the Steele et al. (2017) mesoscale model  
 350 appear to produce higher but still reasonable RH and vmr at Curiosity during the night, but  
 351 somewhat too high vmr during the day compared to the ChemCam and local CRISM vmr results.  
 352 This may mean that the air within the crater is locally dry during daytime. On the other hand, if  
 353 adsorption is switched off in these models, RH and vmr remain much too high during the night.  
 354 Furthermore, this leads to formation of frost at the MSL site during the cool season, by both models.  
 355 Frost has not been observed along the Curiosity track so far (Martinez et al., 2016, 2017).

356

357 We next discuss the vertical structure of moisture at Gale. Figure 8 displays the midday vmr profiles  
 358 for the MSL site from MCD at Ls 90° and 270° (scaled by a constant factor (0.38, 0.54) at all  
 359 heights to match the local ChemCam-observed PWC of Figures 3-4). Shown are also the respective

360 ‘well-mixed’ and ‘low moist layer’ vmr profiles. At Ls 270° the GCM-based MCD indicates warm-  
 361 season moisture well mixed to high altitudes, displaying a broad maximum at about 35 km height.  
 362 In contrast, at Ls 90° a sharp cool-season maximum of moisture is seen at about 10 km height, with  
 363 rapid decay aloft. Most importantly, in both seasons the MCD profiles display relatively low values  
 364 of vmr near the surface. These low values are due to Hadley circulation, which near the surface  
 365 transports the dryness of the respective winter hemisphere to the equatorial latitudes (e.g. Fig.  
 366 11.18, Montmessin et al., 2017). According to MCD data the near-surface dryness dominates  
 367 throughout the year at the MSL site, except at the peak of the moist season (which was not sampled  
 368 by the present ChemCam sky scans).

369  
 370 Some interesting matters can be deduced from Figure 8. Assuming that the MCD profiles are close  
 371 to truth, at Ls 270° the well-mixed assumption is relatively valid for vmr. At the surface it gives an  
 372 estimate just 6% higher than MCD. On the other hand the low moist layer assumption is clearly no  
 373 good during the warm season; at the surface it leads to a large overestimate of about 35%. For Ls  
 374 90° during the cool season, the low moist layer profile appears at first sight better in general than  
 375 the well-mixed one. However, at the surface it does overestimate MCD by about 20%, whereas the  
 376 well-mixed profile is again quite good at the very surface, underestimating MCD there by only  
 377 about 5%.

378  
 379 Thus, due to the fortunate Hadley cell effect, the simple assumption of vertically fully well-mixed  
 380 moisture manages to produce a fairly good estimate for midday surface-vmr at the MLS site (but  
 381 note that this is only valid due to the equatorial latitude!). Therefore the ChemCam well-mixed vmr  
 382 is probably not far from the true daytime surface vmr at Curiosity throughout most of the martian  
 383 year. Our well-mixed model’s daytime vmr (\*) is in turn fairly close to the ChemCam vmr (the  
 384 filled circles) in Figures 5-6, especially during the warm season. In contrast, the low moist layer  
 385 simulations (+) produce large overestimates to the ChemCam vmr during the warm season, being  
 386 closer to them during the cool season. Hence our idealized modeling results and the REMS-H and  
 387 ChemCam observations give support to the seasonally varying vertical distribution of moisture and  
 388 a dry lower equatorial atmosphere as predicted by the GCM experiments.

## 389 390 391 **7. Conclusion**

392  
 393 The local column precipitable water contents from MSL ChemCam passive sky scan retrievals  
 394 (McConnochie et al., 2018) were used to force a local atmosphere-subsurface column model. The  
 395 113 scans covered more than a martian year. ChemCam estimates for the water vapor volume  
 396 mixing ratio (assuming well-mixed moisture) and REMS-H hourly observations of air temperature,  
 397 relative humidity and vmr at 1.6 m height were compared with model results. The sol-to-sol PWC-  
 398 conserving porosity of the regolith turned out to be about 30% in the present model framework.

399  
 400 The REMS-H observations point to a decrease of vmr (i.e. depletion of near-surface water vapor)  
 401 every evening and night throughout the year. The same was observed at the polar Phoenix site in  
 402 summer (Zent et al., 2016), suggesting a global process. If adsorption is allowed, the model’s pre-  
 403 dawn results are quite similar to REMS-H values of T, RH and vmr throughout the year. The  
 404 indicated night depletion ratio is about 0.25 at all seasons. If adsorption is not allowed, RH and vmr  
 405 become excessive during every night at all seasons compared to the REMS-H values, leading to  
 406 surface frost every night between Ls 82°-146°. Frost has not been observed. As brine formation has  
 407 been shown to be unlikely along the Curiosity track, adsorption hence appears to be the main  
 408 depleting process.

409  
 410 The REMS-H vmr values are unfortunately unreliable during the day but the daytime ChemCam  
 411 vmr estimates are available. They appear to be close to the midday surface-vmr from the GCM-



412 based Mars Climate Database profiles for the MLS site (scaled to the ChemCam PWC) during all  
 413 seasons. The well-mixed model's daytime near-surface vmr is in turn close to the respective  
 414 ChemCam vmr throughout the year, whereas simulations with a low moist layer (15 km) lead to  
 415 large overestimates during the warm season, being nearer to the ChemCam vmr during the cool  
 416 season. Higher TES/CRISM-like regional PWC leads to even larger daytime overestimates  
 417 throughout the year, although the nighttime values for RH and vmr remain reasonable. Hence the  
 418 crater appears drier at daytime than the surrounding areas, and the results support a seasonally  
 419 varying vertical distribution of moisture with a dry lower atmosphere, as suggested by GCM  
 420 experiments.

421  
 422

423 **Acknowledgements:** The work was supported by the Academy of Finland grants 131723, 132825  
 424 and 310509. We thank Pierre-Yves Meslin and an anonymous reviewer for good comments, which  
 425 helped to improve the article.

426  
 427

#### 428 **References:**

429

430 Fischer E, Martinez GM, Renno NO, 2018. The Phoenix Lander's relative humidity sensor  
 431 recalibration: new results and analysis. 49<sup>th</sup> Lunar and Planetary Science Conference 2018, LPI  
 432 Contrib. No. 2083.

433

434 Gómez-Elvira GJ et al., 2012. REMS: The Environmental Sensor Suite for the Mars Science  
 435 Laboratory Rover. *Space Sci. Rev.* 170, 583-640, doi:10.1007/s11214-012-9921-1.

436

437 Harri AM, et al., 2014a. Mars Science Laboratory relative humidity observations: initial results. *J.*  
 438 *Geoph. Res. Planets* 119, 2132-2147, doi: 10.1002/2013JE004514

439

440 Harri AM, et al., 2014b. Pressure observations by the Curiosity rover: initial results. *J.Geophys.Res.*  
 441 *Planets* 119, 82-92. doi: 10.1002/2013JE004423.

442

443 Hudson TL, Aharonson O, Schorghofer N, Farmer CB, Hecht MH, Bridges NT, 2007. Water vapor  
 444 diffusion in Mars subsurface environments. *J.Geophys.Res.* 112, E05016.

445

446 Jakosky BM, Zent AP, Zurek RW, 1997. The Mars water cycle: Determining the role of exchange  
 447 with the regolith. *Icarus* 130, 87-95.

448

449 Martínez GM, Fischer E, Rennó NO, Sebastián E, Kempainen O, Bridges N, Borlina CS, Meslin  
 450 PY, Genzer M, Harri AM, Vicente-Retortillo A, 2016. Likely frost events at Gale crater: analysis  
 451 from MSL/REMS measurements. *Icarus* 280, 93–102.

452

453 Martínez GM, Newman CN, De Vicente-Retortillo A, Fischer E, Renno NO, Richardson MI, Fairén  
 454 AG, Genzer M, Guzewich SD, Haberle RM, Harri AM, 2017. The Modern Near-Surface Martian  
 455 Climate: A Review of In-situ Meteorological Data from Viking to Curiosity. *Space Sci. Rev.* pp.1-  
 456 44.

457

458 Martin-Torres FJ, et al., 2015. Transient liquid water and water activity at Gale crater on Mars. *Nat.*  
 459 *Geosci.* 8, 357-361, doi:10.1038/NGEO2412.

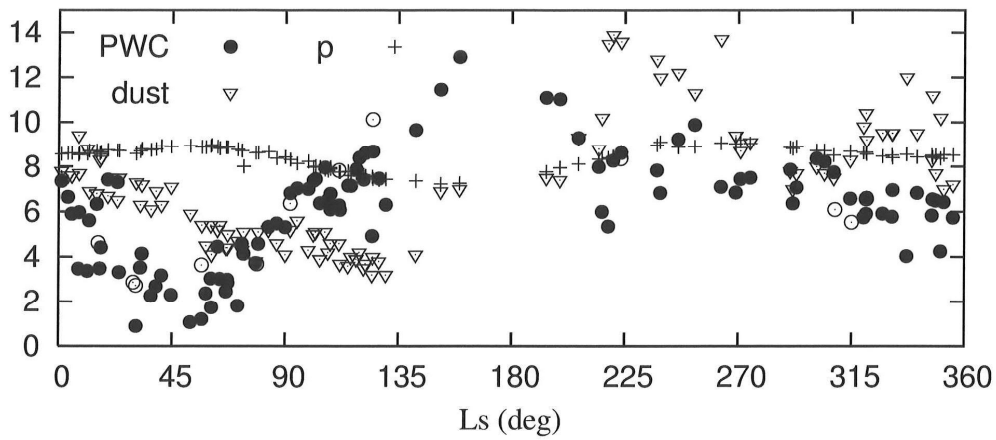
460

461 McConnochie TH, et al., 2018. Retrieval of water vapor column abundance and aerosol properties  
 462 from ChemCam passive sky spectroscopy. *Icarus* 307, 294-326, doi:10.1016/j.icarus.2017.10.043.

463

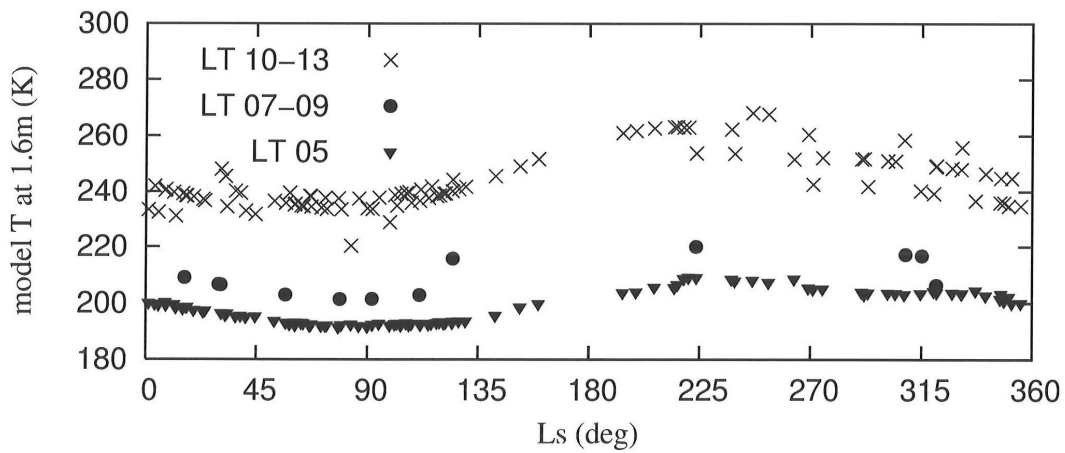
- 464 Millour E et al., 2015. The Mars Climate Database (MCD version 5.2). EPSC2015-438.  
465
- 466 Montmessin F, Smith MD, Langevin Y, Mellon MT, Fedorova A, 2017. The water cycle, pp 338-  
467 373. In "The Atmosphere and Climate of Mars", Haberle RM, Todd Clancy R, Forget F, Smith MD,  
468 Zurek RW, eds. Cambridge University Press, 644 pp.  
469
- 470 Navarro T, et al., 2014. Global climate modeling of the Martian water cycle with improved  
471 microphysics and radiatively active water ice clouds. *J.Geophys.Res.Planets* 119, 1479-1495.  
472
- 473 Richardson MI, Wilson RJ, 2002. Investigation of the nature and stability of the martian seasonal  
474 water cycle with a general circulation model. *J.Geophys.Res. (Planets)* 107.  
475 doi:10.1029/2001JE001536. 7-1.  
476
- 477 Rivera-Valentin EG, Gough RV, Chevrier VF, Primm KM, Martinez GM, Tolbert M, 2018.  
478 Constraining the potential liquid water environment at Gale crater, Mars. *J.Geophys.Res. (Planets)*,  
479 doi:10.1002/2018JE005558.  
480
- 481 Savijärvi H, Määttänen A, 2010. Boundary-layer simulations for the Mars Phoenix lander site.  
482 *Quart. J. Roy. Meteor. Soc.* 136, 1497-1505, doi:10.1002/qj.650  
483
- 484 Savijärvi H, Harri AM, Kempainen O, 2015. Mars Science Laboratory diurnal moisture  
485 observations and column integrations. *J.Geophys.Res. Planets* 120, 1011-1021, doi:  
486 10.1002/2014JE004732  
487
- 488 Savijärvi H, Harri AM, Kempainen O, 2016. The diurnal water cycle at Curiosity: role of exchange  
489 with the regolith. *Icarus* 265, 63-69, doi:10.1016/j.icarus.2015.10.00  
490
- 491 Savijärvi H, Paton M, Harri AM, 2017: New column simulations for the Viking landers: winds, fog,  
492 frost, adsorption? *Icarus*, doi: 10.1016/j.icarus.2017.11.007.  
493
- 494 Steele LJ, Lewis SR, Patel MR, Montmessin F, Forget F, Smith MD, 2015. The seasonal cycle of  
495 water vapor on Mars from assimilation of thermal emission spectrometer data. *Icarus* 237, 97-115.  
496
- 497 Steele LJ, Balme MR, Lewis SR, Spiga A, 2017. The water cycle and regolith-atmosphere  
498 interaction at Gale crater, Mars. *Icarus* 280, 56-79.  
499
- 500 Toigo AD, Smith MD, Seelos FP, Murchie SL, 2013. High spatial and temporal resolution sampling  
501 of Martian gas abundances from CRISM spectra. *J.Geophys.Res., Planets* 118, 89, doi:  
502 10.1029/2012JE004147.  
503
- 504 Zent AP, Hecht MH, Hudson TL, Wood SE, Chevrier VF, 2016. A revised calibration function and  
505 results for the Phoenix mission TECP relative humidity sensor. *J. Geophys. Res. (Planets)* 121, 626-  
506 651.

508  
509  
510  
511



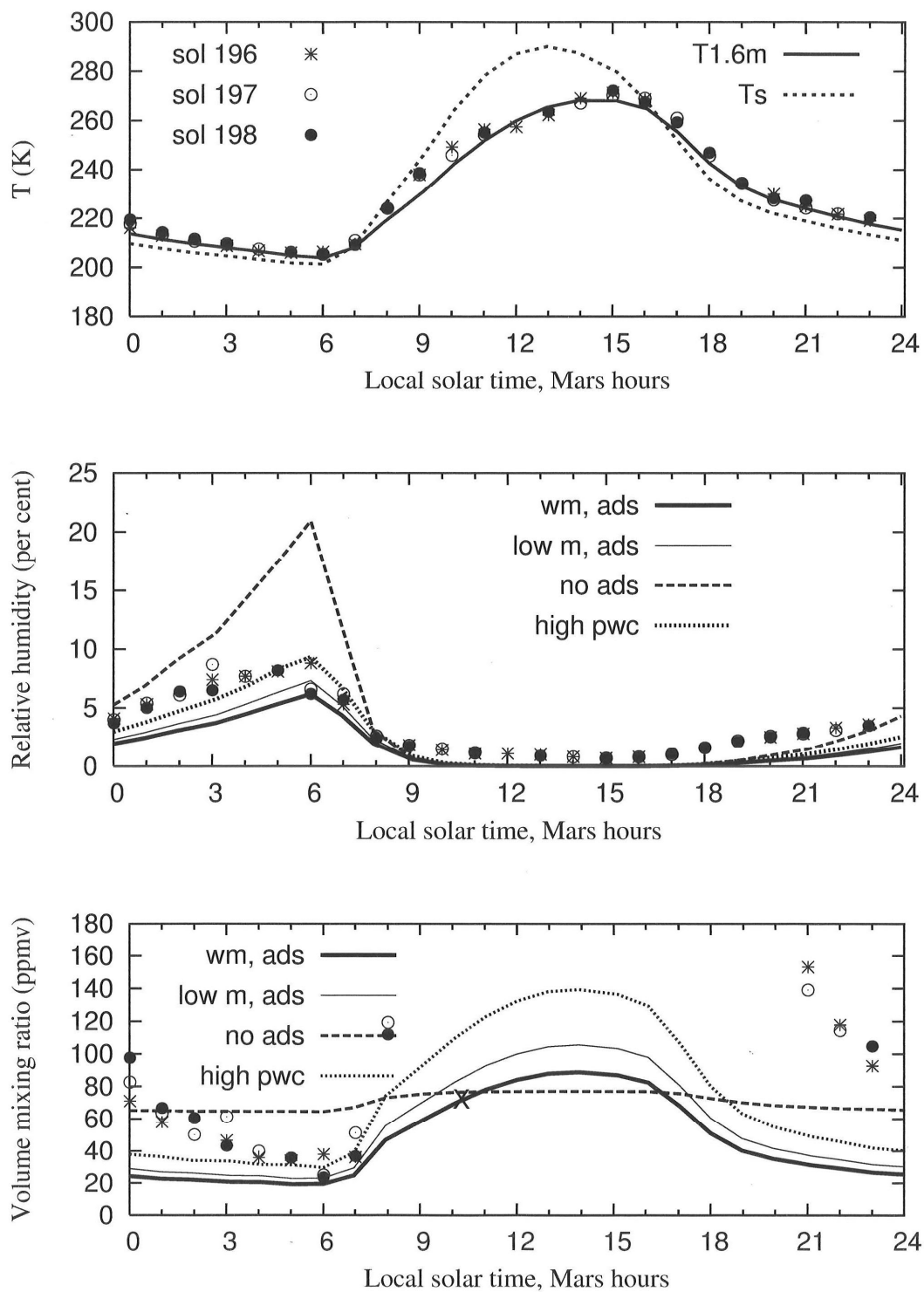
512  
513  
514  
515  
516  
517  
518  
519

Figure 1. Column precipitable water content (PWC, in  $\mu\text{m}$ ) from MSL ChemCam passive sky scans (filled circles from daytime, open circles from morning), column total opacity, mostly by dust ( $\tau$  multiplied by 10) from MSL MastCam, and surface pressure (p, in mb) from MSL REMS-P.



520  
521  
522  
523  
524

Figure 2. Model 1.6 m temperatures at 05:00LT and at the nearest hour (e.g. 11:00LT) for each ChemCam PWC observation of Figure 1.



525  
 526  
 527  
 528  
 529  
 530  
 531  
 532  
 533  
 534  
 535  
 536

Figure 3. Hourly REMS-H observations (marks) for three sols at around Ls 271° during the warm season, and model results in the four experiments (lines). Top panel: T1.6 m and Ts. Mid panel: Relative humidity at 1.6 m. Bottom panel: Volume mixing ratio at 1.6 m; X is the ChemCam vmr observation. REMS RH and vmr values are considered unreliable during 08-21LT due to low RH.

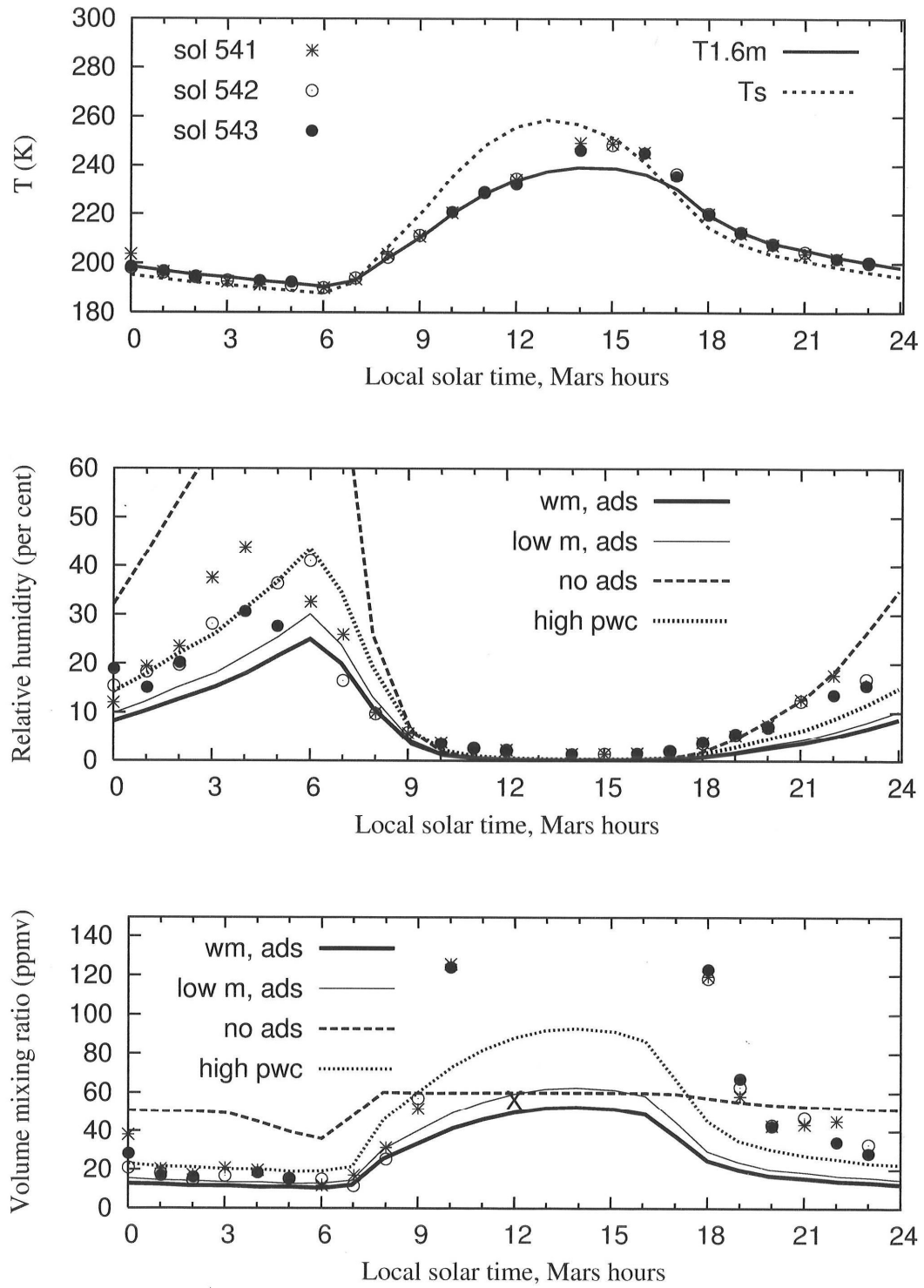
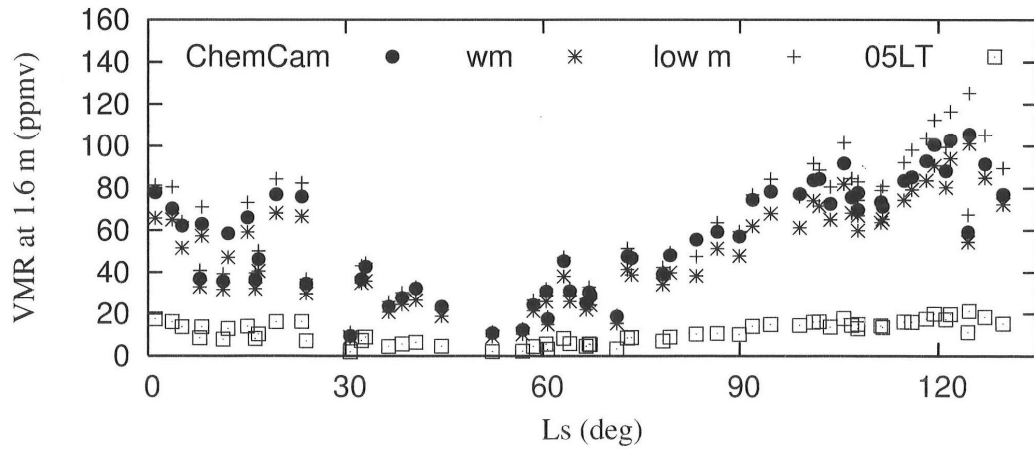


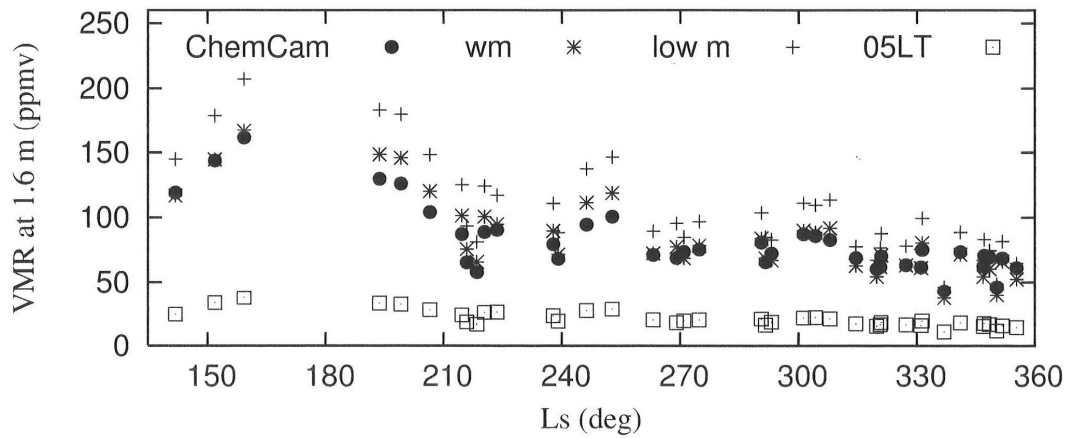
Figure 4. As Figure 3 but for the cool season, at around Ls 90°.

537  
538  
539  
540  
541  
542  
543  
544  
545  
546  
547  
548



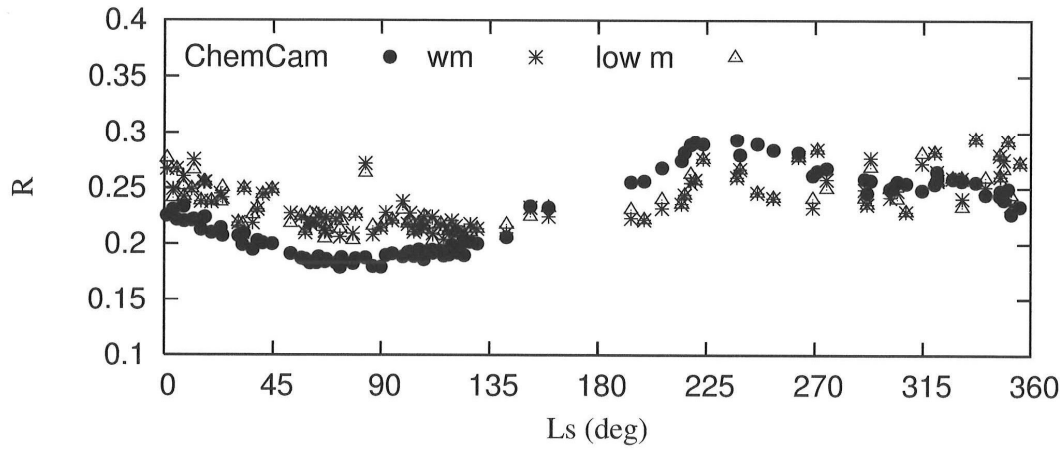
549  
550  
551  
552  
553  
554  
555  
556  
557

Figure 5. The cool season ( $L_s$   $0^\circ$ - $135^\circ$ ) volume mixing ratios from all ChemCam daytime scans (filled circles); model 1.6 m vmr at the scan time (well-mixed simulation \*, low moist layer simulation +), and at 05LT (squares). The  $L_s$   $90^\circ$  case was shown in Figure 4.



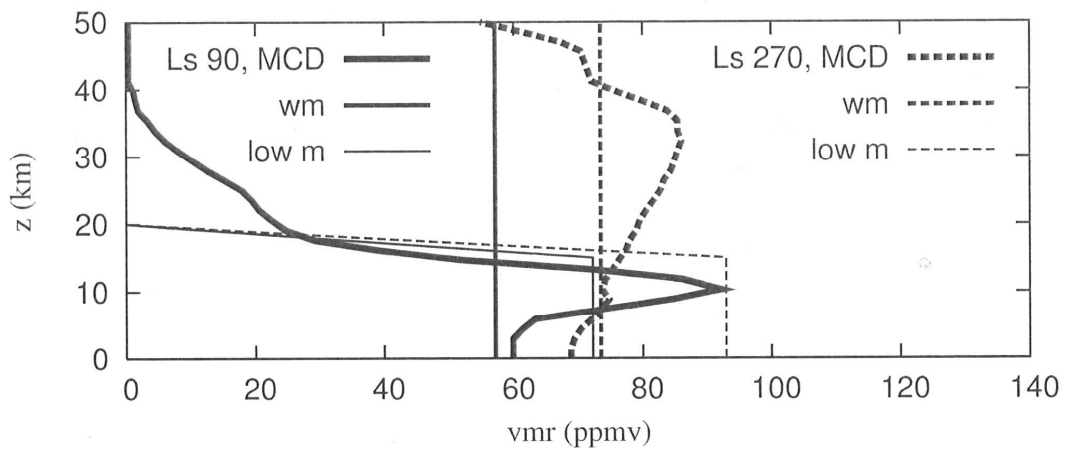
558  
559  
560  
561  
562  
563

Figure 6. As Figure 5 but for the moist and warm seasons,  $L_s$   $135^\circ$ - $360^\circ$ . The  $L_s$   $271^\circ$  case was shown in Figure 3.



564  
565  
566  
567  
568  
569  
570  
571  
572  
573

Figure 7. The night depletion ratio  $R$  ( $\text{vmr}(05\text{LT})/\text{vmr}(\text{daytime})$ ) using the ChemCam vmr and the model 1.6 m vmr from Figures 5-6 (well mixed simulation: stars, low moisture layer simulation: triangles). The 05LT value for ChemCam  $R$  is from the well-mixed simulation.



574  
575  
576  
577  
578

Figure 8. 12LT volume mixing ratio profiles (scaled to ChemCam PWC) at the MSL site for  $L_s 90^\circ$  and  $L_s 270^\circ$  from the GCM-based Mars Climate Database (MCD), and the respective same-PWC profiles for the well-mixed (wm) and low moist layer (low m) assumptions.